Response of High-Rise and Base-Isolated Buildings to a Hypothetical M_W 7.0 Blind Thrust Earthquake

Thomas H. Heaton, John F. Hall, David J. Wald, Marvin W. Halling*

High-rise flexible-frame buildings are commonly considered to be resistant to shaking from the largest earthquakes. In addition, base isolation has become increasingly popular for critical buildings that should still function after an earthquake. How will these two types of buildings perform if a large earthquake occurs beneath a metropolitan area? To answer this question, we simulated the near-source ground motions of a M_W 7.0 thrust earthquake and then mathematically modeled the response of a 20-story steel-frame building and a 3-story base-isolated building. The synthesized ground motions were characterized by large displacement pulses (up to 2 meters) and large ground velocities. These ground motions caused large deformation and possible collapse of the frame building, and they required exceptional measures in the design of the base-isolated building if it was to remain functional.

The 17 January 1994 Northridge earthquake (M_w 6.7) (*1*) demonstrated the importance of earthquakes on blind thrust faults beneath heavily urbanized areas of southern California. Even larger earthquakes have occurred in similar tectonic regions (*2*), and analysis of the geologic structure beneath Los Angeles is compatible with the occurrence of thrust earthquakes as large as M_w 7.5, with average recurrence intervals of several hundred years (*3*). Furthermore, other urban areas are certain to experience near-source ground motions from future large earthquakes. In particular, the San Francisco Bay area not only experienced a devastating M_w 7.8 earthquake in 1906 on the San Andreas fault, but it also experienced earthquakes of about M_w 7 on the Hayward fault in 1836 and 1868. The 30-year probability of another San Francisco Bay area earthquake of M_w 7.0 or larger has been estimated to be about 67% (*4*).

Flexible-frame buildings are generally considered to be earthquake resistant because they are thought to attract less seismic force into the building frames than do more rigid buildings with braced frames or shear walls. Also, the construction of buildings on rubber pads (base isolation) is an increasingly popular way to reduce damage to structures and their contents by decreasing the accelerations transmitted to buildings. The actual performance of these design techniques during near-source ground motions from very large earthquakes has not been directly tested, because no earthquake larger than the recent M_w 6.7 Northridge earthquake has occurred directly beneath a major metropolitan region. However, the occurrence of urban earthquakes larger than M_w 7.0 is inevitable.

In this report, we describe models of ground motions produced by fault slips similar to those inferred for the 1992 Landers, California, earthquake (M_w 7.2) and the use of these models to predict the performance of a 20-story steel-frame building and a 3-story base-isolated building.

There are relatively few near-source ground-motion recordings of large earthquakes. However, the existing records demonstrate the violent nature of the shaking that often occurs. The median peak acceleration and velocity of 27 recordings at distances of 5 km or less from the surface projection of the rupture surface for earthquakes of $M_w \geq 6.5$ are 0.81*g* and 102 cm/s, respectively (Table 1). In two instances, the

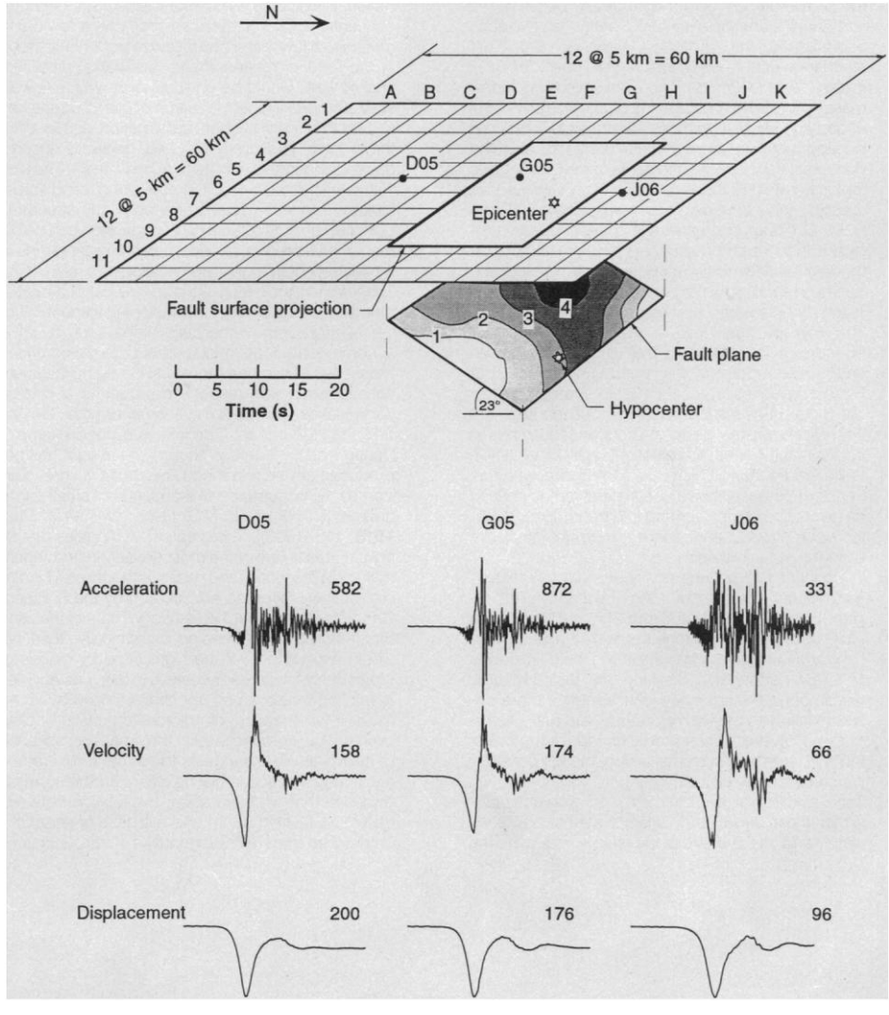

Fig. 1. Assumed rupture surface for a hypothetical M_W 7.0 earthquake. The star is the assumed hypocenter-epicenter. Contours of slip in meters are similar to those used to model slip on the Homestead Valley segment of the 1992 M_W 7.2 Landers earthquake (*11*). The rupture surface dips 23° to the north, and the bottom and top of the rupture surface are at 16 and 9 km, respectively. Ground motions are modeled at each of the grid points. The predicted ground acceleration (cm/s^2), velocity (cm/s), and displacement (cm) are also shown for selected sites and for the component having the largest peak-to-peak velocity. N6°E for D05, N33°W for G05, and N74°W for J06.

peak acceleration exceeded the range of the accelerometer. The listed peak displacements often underestimate the actual displacements because high-pass filters are normally applied. One exception is the displacement from the Landers earthquake, which was calculated with techniques designed to preserve the true long-period displacements (5).

We expect that M_w 7.5 earthquakes will produce near-source peak accelerations that are only modestly larger than those from M_w 6.5 earthquakes (perhaps 25% larger) (6). However, this is not the case at longer periods. As the magnitude grows from 6.5 to 7.5, the average fault slip increases by a factor of 3.16 and the rupture area increases by a factor of 10 (7). Thus, peak near-source displacements are expected to increase strongly with magnitude, although reliably processed data are still too few to provide a quantitative estimate. Also, displacements must be quite large close to large earthquakes, because observed fault offsets have exceeded 5 m. Furthermore, these large slips usually occur in less than several seconds (8).

For periods ≥1 s, near-source ground motions are strongly affected by directivity. That is, because ruptures propagate at about 85% of the shear-wave velocity, the amplitudes of direct shear-wave arrivals become large along the direction of propagation (9). Furthermore, the shear wave in the direction of rupture propagation usually consists of a large pulse with an amplitude comparable to that of the fault slip and a duration comparable to the duration of slip for any given point on the fault. In the near-source region, large peak ground velocities are often associated with this pulse, particularly within 10 km of the rupture surface.

Near-source ground motions at periods greater than 1 s have been successfully modeled for at least 10 California earthquakes (10). The success of these modeling studies makes us confident that longer period near-source ground motions can be predicted for future hypothetical earthquakes.

For this study, we estimated strong ground motions within the frequency bandwidth of 0.0 to 10.0 Hz for a hypothetical M_w 7.0 earthquake (M_0 = 3.96 × 10^{26} dyne · cm) on an east-west trending blind thrust that dips 23° northward beneath a sedimentary basin. The assumed rupture surface was 35 km long and 18 km wide (Fig. 1); the faulting was confined to depths between 9 and 16 km; the hypocenter was assumed to be in the lower center of the fault; and the rupture velocity was 2.9 km/s. The dimensions of this rupture are compatible with those of a large earthquake on the north-dipping Elysian Park blind thrust fault that lies directly beneath Los Angeles (3) and was the apparent source of the M_w 5.9 1987 Whittier Narrows earthquake.

This hypothetical earthquake is only one of many that can be suggested for the Los Angeles metropolitan region. Although larger earthquakes could be hypothesized, a M_w 7.0 earthquake seems reasonable for several thrust systems, especially considering the recent occurrence of the M_w 6.7 Northridge earthquake.

In the model, ground motions were deterministically calculated at periods longer than 1 s, whereas at shorter periods, ground motions were approximated by actual recordings of acceleration in other earthquakes. That is, we used a matched pair of filters to remove short periods from our deterministic synthetics and to remove long periods from actual recorded ground motions. The filtered records were then summed to form the final ground motion. The short-period part of the motions was recorded at Olive View hospital and Stone Canyon reservoir (peak horizontal accelerations of 0.90*g* and 0.38*g*, respectively) during the 1994 Northridge (M_w 6.7) earthquake. We corrected these records for the appropriate distance using the attenuation relations of Boore, Joyner, and Fumal (6). The Olive View records were used to simulate motions for stations located in the direction of rupture (all stations south and west of G06 in Fig. 1), and the Stone Canyon records were used for all other sites.

We calculated the long-period part of the ground motion by assuming that variable slip occurred on the fault plane; we used the slip variations determined for the Homestead Valley segment of the M_w 7.2 1992 Landers earthquake (11) (Fig. 1). However, we increased the rupture area by a factor of 1.4 and decreased the slip by a factor of 0.74 so that rupture area and the average slip (2.2 m) were near that expected for a M_w 7.0

Table 1. Peak near-source ground motions from large earthquakes. Distance is the approximate horizontal distance from the recording site to the surface projection of the rupture; acceleration, velocity, and displacement are the observed peak ground acceleration, velocity, and displacement, respectively.

Earthquake	Distance (km)	Acceleration (*g*)	Velocity (cm/s)	Displacement (cm)
1979 Imperial Valley, USA, M_w 6.5				
El Centro Array 7	1	0.65	110	41
El Centro Array 6	1	1.74	110	55
Bonds Corner	4	0.81	44	15
El Centro Array 5	4	0.56	87	52
El Centro Array 8	4	0.64	53	29
1987 Superstition, USA, M_w 6.6				
Parachute Test site	0	0.53	138	60
Superstition Mountain	6	0.91	44	15
1971 San Fernando, USA, M_w 6.7				
Pacoima Dam	0	1.12	113	38
1994 Northridge, USA, M_w 6.7				
Rinaldi	0	0.85	177	50
Sylmar	0	0.90	129	50
Los Angeles Dam	0	0.32	79	22
Sylmar County Hospital	2	0.91	134	44
Van Nuys (hotel)	2	0.47	48	13
Arleta fire station	4	0.59	44	15
Newhall fire station	5	0.63	101	36
Tarzana nursery	5	1.82		
Sepulveda Veterans Hospital	0	0.94	75	15
Jensen Filtration Plant	0	0.85	103	38
1985 Nahanni, Canada, M_w 6.8				
Site 1	0	>2.0	39	36
Site 2	0	0.50	31	31
1992 Erzincan, Turkey, M_w 6.8				
Erzincan	2	0.50	105	40
1989 Loma Prieta, USA, M_w 6.9				
Lexington Dam	5	0.44	120	32
Los Gatos Presentation Center	0	0.62	102	40
1992 Petrolia, USA, M_w 7.0				
Cape Mendocino	0	>1.8	126	67
Petrolia	5	0.69	90	31
1993 Landers, USA, M_w 7.2				
Lucerne	1	0.90	142	255
1978 Tabas, Iran, M_w 7.4				
Tabas	3	0.92	125	106

T. H. Heaton and D. J. Wald, U.S. Geological Survey, 525 South Wilson Avenue, Pasadena, CA 91106, USA.
J. F. Hall and M. W. Halling, Earthquake Engineering Research Laboratory, California Institute of Technology, Pasadena, CA 91125, USA.

*Present address: Department of Civil and Environmental Engineering, Utah State University, Logan, UT 84322–4110, USA.

earthquake. The peak slip in this model was 5.1 m. Slip at each point was characterized by Brune's (*12*) source function, and we scaled the slip duration for each point on the fault so that the particle velocity was near 1 m/s. We used the discrete-wavenumber finite-element technique (*13*) to calculate the response of point dislocations in a vertically stratified crustal model that approximates the average seismic velocities in the Los Angeles basin. For periods longer than 1 s, this procedure produced the complete solution for a finite rupture embedded in a layered half-space.

We computed ground motion time histories on a rectangular grid of sites (11 by 11 with a 5-km spacing) (Fig. 1). The largest ground motions were south of the fault (peak displacement of 200 cm at D05; peak velocity of 177 cm/s at H05), where directivity dominates the ground motions (Fig. 2, A and B).

How realistic are these synthetic ground motions? Because the high-frequency parts of the records were actually recorded in a M_w 6.7 earthquake, the peak accelerations are plausible. Peak acceleration, however, is probably less important than the peak velocities and displacements when considering the response of buildings with long natural periods of vibration. Large velocities and displacements at near-source sites inevitably result from the large slips that occur during high-magnitude earthquakes. Comparably large velocities were recorded in the 1994 Northridge and 1992 Landers earthquakes, and even larger displacements can be inferred for a site located close to the 1992 Landers earthquake (Table 1). In our model, the average peak velocity for sites within 5 km of the surface projection of the rupture surface is 81 cm/s, which is somewhat lower than the 102 cm/s median of peak velocities listed in Table 1.

One potential deficiency of our model is that we do not include the three-dimensional effects of wave propagation in a basin (such as the Los Angeles basin). We anticipate that the duration of ground shaking would increase if multiply reflected body and surface waves within a basin were included. The near-source ground motions are still likely to be dominated by direct shear waves, which are controlled primarily by source radiation and directivity effects, which are well modeled with our procedures. However, for earthquakes with shallow rupture or larger source dimensions, inclusion of effects from wave propagation in basins may be extremely important.

Our synthetic ground motions contained a large pulse of displacement. Such large pulses have been commonly observed in the near-source region of earthquakes, and they are caused by directivity, which is the inevitable result of rupture propagation velocities that are close to the shear-wave velocity. These pulses are important because they account for most of the radiated kinetic energy from an earthquake. Furthermore, these pulses are not adequately represented in modern codes for conventional fixed-base buildings, because these codes are based mostly on experience from smaller earthquakes. Although a few previous studies have demonstrated the damaging effects of near-source ground motions (*14, 15*), the issue is not widely appreciated in the engineering community, especially for earthquakes larger than M_w 7.0.

We developed a model of a 20-story building (Fig. 3) with a symmetric steel-frame structure constructed of I-section vertical columns and horizontal beams. Those on the exterior faces of the building are joined together rigidly to give the building lateral strength and stiffness to resist wind and earthquake forces. The design is according to the 1991 Uniform Building Code (*16*) for gravity loads, wind forces, and earthquake forces (Zone 4, deep stiff soil). Zone 4 has the highest seismic requirements, and it is the intention of the code to prevent collapse during ground motions having an "intensity equal to the strongest either experienced or forecast for the building site" (*17*), which has been quantified as a 500-year event. According to the code, damage may occur during this event, but it is expected to be repairable.

In the simulation, the component of ground motion that maximizes peak-to-peak ground velocity was applied in the direction parallel to the short direction of the building. The structure was regarded as five planar frames (two exterior and three interior; Fig. 3) connected by floor slabs. Twisting was neglected and symmetry was used to halve the model. The exterior frame (Fig. 3) was represented mathematically in detail, whereas the interior frames, which were designed to carry only vertical loads, were included in a simpler form. To account for incidental lateral resistance from the interior frames and other sources, interstory shear springs were added between adjacent floors. The spring in the below-ground story also represents stiff basement walls. The additional lateral strength provided to the building by the shear springs amounts to 30% of the code design force. There are also axial springs mounted horizontally and vertically at the base of each column to account for foundation flexibility. In the elastic range, the building has a period of 3.9 s. Viscous mechanisms were incorporated to

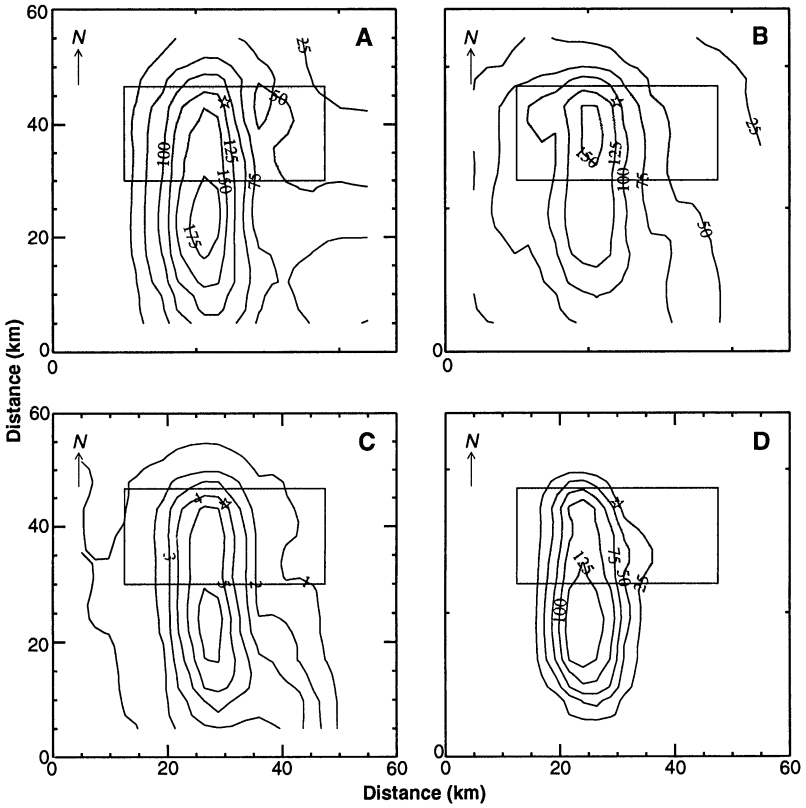

Fig. 2. Spatial distribution of peak shaking parameters for the grid and rupture model from Fig. 1. The rectangular box is the surface projection of the rupture, and the star is the epicenter. (**A**) Peak horizontal ground displacement (cm). (**B**) Peak horizontal ground velocity (cm/s). (**C**) Percent drift in the first story of the 20-story building. (**D**) Velocity of collision (cm/s) between three-story base-isolated building and its stop if the stop is at a pad displacement of 40 cm.

provide a light amount of damping (2% of critical) (*18*).

The nonlinear features of the exterior-frame model (*19*) include inelastic behavior in the beams and columns for axial stress and in the panel zones for shear stress. We used realistic stress-strain hysteretic curves for steel (yield and ultimate strengths of 290 MPa and 448 MPa, respectively). The interstory shear springs were modeled as elastic-plastic elements, and we also included yielding in the foundation. Geometric nonlinearity from the changing building configuration during its earthquake response was fully modeled. Notable limitations include the lack of a full accounting for three-dimensional effects and the absence of mechanisms of structural degradation.

The responses of the 20-story building are shown in Fig. 2C as contours of story drift (peak story sway as a percentage of the story height) for the first story. Whereas a story drift of 2% is considered severe, the first-story drift exceeded 6% (corresponding to 35 cm of sway) at sites D05, E05, and E06, and it exceeded 2% at 40 sites (covering a region of 1000 km^2). Displacement time histories for site D05 (Fig. 4, solid lines) show that large offsets developed in several lower stories. The results indicate that the ground motion most damaging to a multistory building is a rapid pulse motion, forward and back, which is timed so that the backward phase strikes the building just as it has acquired a large forward velocity (Fig. 5).

Although the above results do not show collapse of the building, the deformations are well into the range where structural degradation would occur, such as flange buckling of the I-sections or weld fracture (*20*), and these are difficult to represent accurately in a mathematical model. For a tall building subjected to a large, rapid displacement pulse, tension forces develop in the exterior columns from bending of the building as a cantilevered beam, raising the possibility of a tensile fracture in a column splice. We demonstrated the consequences of such a fracture by repeating the above simulation with column splices in the first above-ground story that fracture when the column tension force reaches an axial strength set to 25% of the yield capacity of the column section (*21*). For the ground motion at site D05, an exterior column broke during the back phase of the ground displacement pulse. Unchecked lateral displacement occurred in the first above-ground story and the building collapsed (Fig. 5, dashed lines), demonstrating the importance of structural degradation mechanisms. Although this is a possible collapse scenario for a tall building subjected to a large, rapid displacement pulse, the benefits of three-dimensional frame action should be studied.

Although the ground motions generated for the M_w 7.0 earthquake would be a strong test for modern buildings of many heights, the 20-story building may be in a height range that is particularly vulnerable. Earthquake design loads in building codes are relatively larger for shorter buildings, and, for taller ones, the design lateral strength is increased because of consideration of wind loads. Although the building we analyzed had a steel frame, reinforced concrete-frame buildings could also be seriously affected by the M_w 7.0 ground motions, because the code design forces are the same for steel and concrete.

We now discuss the implications of our synthesized ground motions for base-isolated buildings. Isolating a building from the motions of its foundation by inserting rubber pads between the two may significantly reduce seismic forces within the building. However, large displacement pulses present a problem because they can produce large pad displacements. The maximum anticipated pad displacements (D_{TM} in Uniform Building Code notation) should be within the range of pad stability. As a precaution, stops (such as concrete walls) are often provided around the base of the building, with a clearance taken here as D_{TM}. The value of D_{TM} should not be underestimated, as a collision with the stops could damage the building.

We considered a three-story base-isolated building with an elastic superstructure whose properties are given in Fig. 6. Three designs, with clearances of 40, 50, and 60 cm, were examined. In all three designs, the building's effective period was

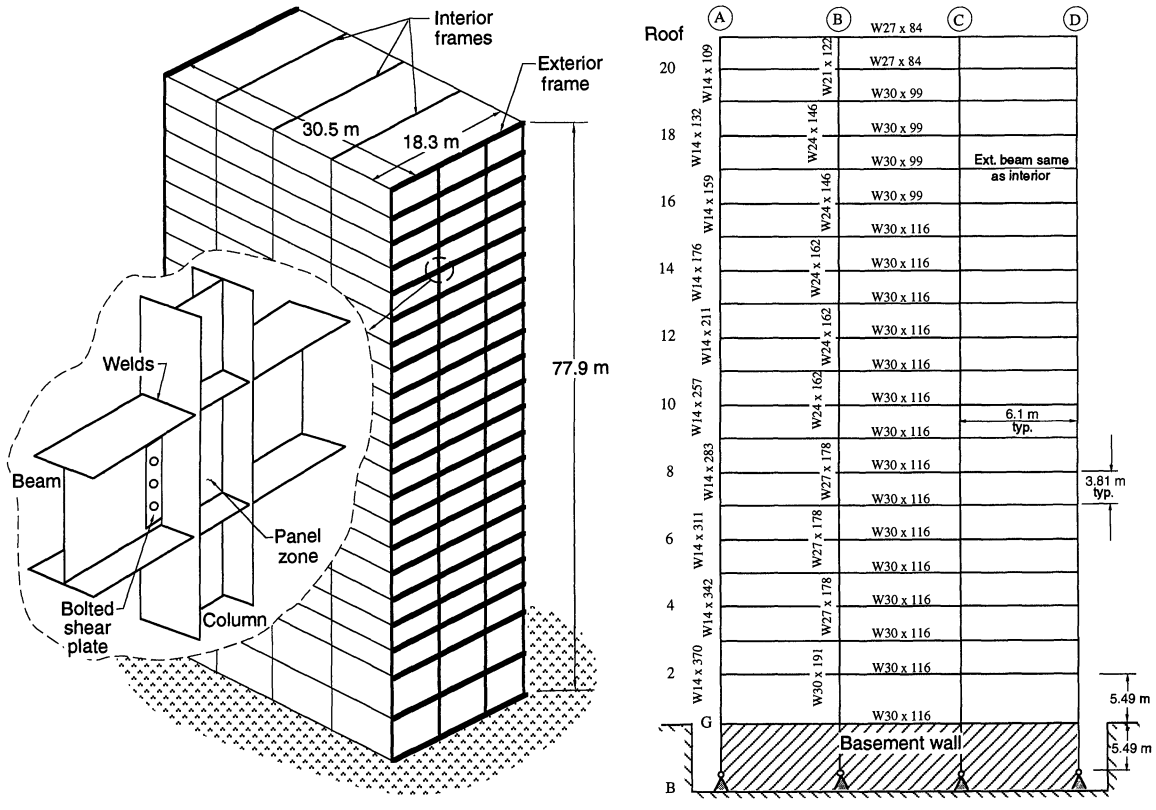

Fig. 3. Twenty-story steel-frame building used in the computer simulation study. (**Left**) Perspective view of the building with detail of a beam-column joint shown in the inset. (**Right**) Details of the end frame at the narrow face of the building. Member designation is according to the American Institute of Steel Construction (*24*).

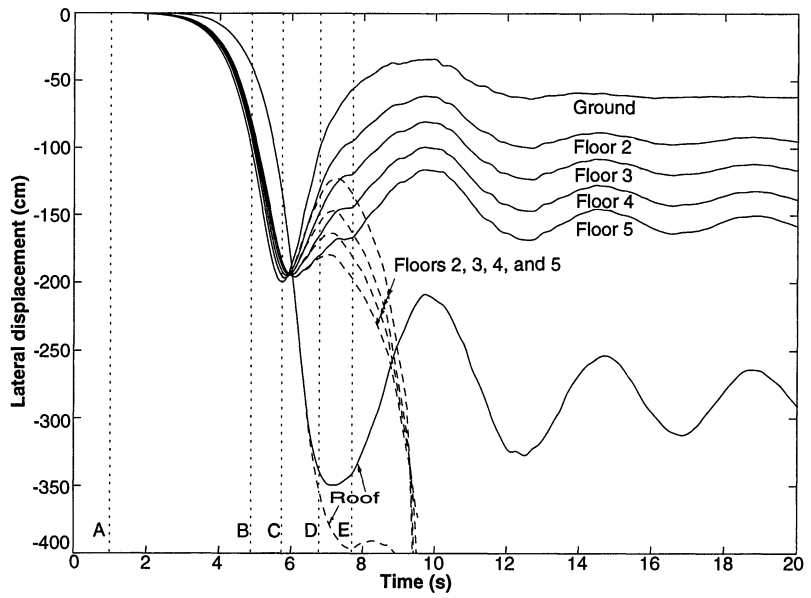

Fig. 4. Plots of lateral displacement time histories of the ground through fifth floors and roof of the 20-story building, resulting from the N6°E component of the D05 ground motion (Fig. 1). Solid lines correspond to a simulation in which no structural degradation occurs (see text). Dashed lines correspond to a simulation that includes structural degradation in the form of weak column splices in the first above-ground story. The times marked A through E correspond to the configurations plotted in Fig. 5 after scaling up the lateral displacements by a factor of 4. When no structural degradation is assumed, severe deformations occur but the building does not collapse. When weak column splices are included, one of the columns ruptures in tension and the building collapses.

2.25 s and the pad's energy dissipative properties were equivalent to viscous damping at 15% of critical (*22*). To reduce pad displacement, designs D_{TM} = 50 cm and D_{TM} = 60 cm had additional viscous damping at the pads that was equal to 5% and 10% of critical, respectively. The D_{TM} = 60 cm design is near the limit of what is currently being designed.

Results of the simulation for the D_{TM} = 40 cm design show that collisions with the stops occurred at 26 of the grid locations (covering a region of 650 km^2), with a maximum striking velocity of 165 cm/s at location D05 (Fig. 2D). Such a high-velocity impact would cause substantial damage to the building. Increasing the clearance to 50 cm and adding 5% damping to the pads reduced the area of collisions to 300 km^2 and the maximum striking velocity to 140 cm/s. Collisions still occurred in a 75-km^2 area for the 60-cm clearance with 10% added damping (maximum striking velocity of 66 cm/s). Although this design eliminated most of the collisions, substantial forces were still transmitted to the building.

The results indicate that: (i) A 40-cm clearance, although greater than that at several existing southern California base-isolated buildings, is much too small for the near-source ground motions from a M_w 7.0 earthquake. (ii) Exceptional measures are required to design a base-isolated building that remains functional for the strongest of ground motions from a M_w 7.0 earthquake.

Although there are relatively few near-source recordings of ground motions from large earthquakes, it is clear that whereas accelerations grow modestly as the earthquake size increases, ground velocities and displacements become quite large. In our modeling, we chose parameters that we felt were typical for a M_w 7.0 earthquake. Unfortunately, it is difficult to put an upper limit on the near-source displacement; peak surficial slips of nearly 10 m have been inferred for the 1857 Fort Tejon, California, earthquake (*23*). Although such large earthquakes are infrequent, it also appears inevitable that an urbanized region of California will experience near-source motions from a very large earthquake.

It is logical that building practice should be based on adequate knowledge of ground motions in large earthquakes and the corresponding response of buildings to those ground motions. However, such knowledge has not been available to earthquake engineers; it is still the subject of basic earth-

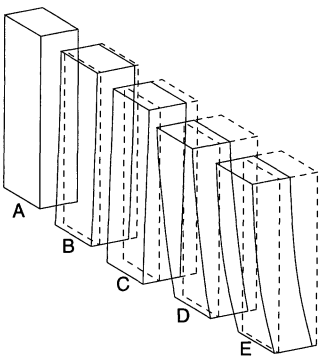

Fig. 5. Illustration of the effect of a forward and back displacement pulse on a multistory building. Dotted lines show the undeformed figure of the building for reference. A: Building is at rest before the pulse arrives. B: Forward phase of the pulse. Building is moving forward but lagging in the upper stories. C: Ground has reached its maximum displacement. Most of the building is moving rapidly forward. D: Back phase of the pulse. Much of the building is still moving forward. E: End of ground displacement pulse. Building is left with a severe forward lean with large offsets in lower stories, or it may be collapsing.

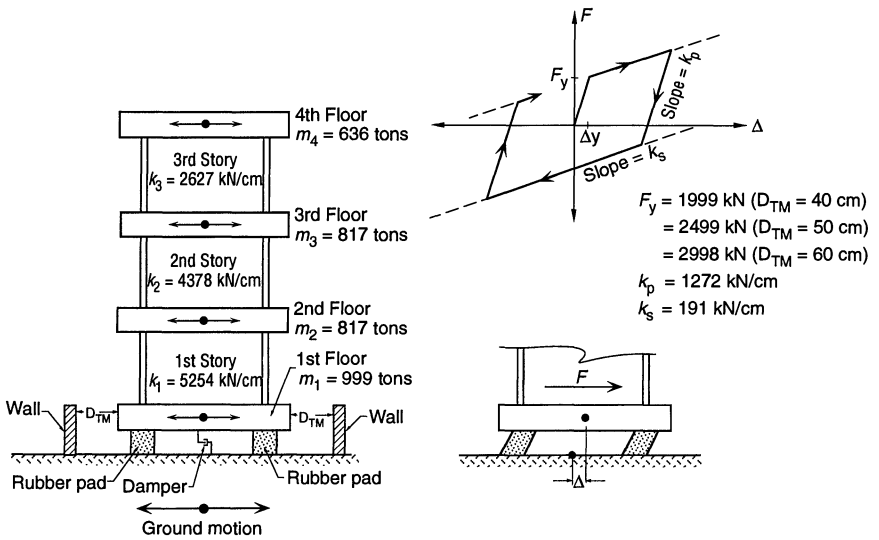

Fig. 6. Idealized three-story building used in the base-isolation study. k_1, lateral story stiffness for story 1; m_1, lumped mass for floor 1. The hysteretic diagram shown is for all rubber pads combined. The pad shearing displacement is Δ, and the shear force carried by the pads is *F*. Allowable pad displacement (D_{TM}) and viscous damping at the pad level are given in the text. The superstructure is damped at 5% of critical.

quake research. For conventional fixed-base buildings, design practice has advanced incrementally as earthquakes occur and lessons are learned. The weakness in this approach is that we have yet to learn the lessons from a very large ($M_w > 7$) earthquake directly beneath an urban area. This is particularly true for tall buildings that are vulnerable to large ground displacements, both for damage and possible collapse.

Designs of base-isolated buildings are based on site-specific ground motions that should account for near-source effects. However, the ground motions presented here are large compared to those currently used for design at sites close to major California faults, and the strongest of our ground motions require exceptional measures for the isolation system to maintain functionality of the building. The practicality of such a goal in the near-source region of a $M_w \geq 7.0$ earthquake is uncertain. Although the focus of this paper is modern buildings, an even greater hazard lies in structures built before modern codes, especially unreinforced or nominally retrofitted brick buildings and nonductile concrete buildings.

REFERENCES AND NOTES

1. M_w is energy magnitude [H. Kanamori, *Tectonophysics* **49**, 207 (1978)], and it is similar to the moment magnitude scale [T. Hanks and H. Kanamori, *J. Geophys. Res.* **84**, 2348 (1979)]. In the range of 6.5 to 7.5, energy magnitudes are also similar to magnitudes as measured on the surface-wave magnitude scale M_S which, in this magnitude range, has often been called the "Richter scale."
2. R. S. Stein and G. C. P. King, *Science* **224**, 869 (1984); R. Stein and R. Yeats, *Sci. Am.* **260**, 48 (June 1989).
3. J. Dolan *et al.*, *Science* **267**, 199 (1995).
4. Working Group on California Earthquake Probabilities, *U.S. Geol. Surv. Circ. 1053* (1990).
5. W. Iwan and X. Chen, in *Proceedings of the 10th European Conference on Earthquake Engineering* (Vienna, Austria, in press).
6. D. Boore, W. Joyner, T. Fumal, *U.S. Geol. Surv. Open-File Rep. 93-509* (1993).
7. H. Kanamori and D. Anderson, *Bull. Seismol. Soc. Am.* **65**, 1073 (1975).
8. T. Heaton, *Phys. Earth Planet. Inter.* **64**, 1 (1990).
9. R. Archuleta and S. Hartzell, *Bull. Seismol. Soc. Am.* **71**, 939 (1981).
10. For the 1971 San Fernando earthquake, see T. Heaton, *Bull. Seismol. Soc. Am.* **72**, 2037 (1982). For the 1979 Imperial Valley earthquake, see S. Hartzell and T. Heaton, *Bull. Seismol. Soc. Am.* **73**, 1553 (1983) and R. Archuleta, *J. Geophys. Res.* **89**, 4559 (1984). For the 1984 Morgan Hill earthquake, see S. Hartzell and T. Heaton, *Bull. Seismol. Soc. Am.* **76**, 649 (1986) and G. Beroza and P. Spudich, *J. Geophys. Res.* **93**, 6275 (1988). For the 1986 North Palm Springs earthquake, see S. Hartzell, *J. Geophys. Res.* **94**, 7515 (1989). For the 1987 Whittier Narrows earthquake, see S. Hartzell and M. Iida, *J. Geophys. Res.* **95**, 12475 (1990). For the 1987 Superstition Hills earthquake, see D. Wald, D. Helmberger, S. Hartzell, *Bull. Seismol. Soc. Am.* **80**, 1079 (1990). For the 1989 Loma Prieta earthquake, see D. Wald, T. Heaton, D. Helmberger, *Bull. Seismol. Soc. Am.* **81**, 1540 (1991); J. Steidl, R. Archuleta, S. Hartzell, *Bull. Seismol. Soc. Am.* **81**, 1573 (1991); and G. Beroza, *Bull. Seismol. Soc. Am.* **91**, 1603 (1991). For the 1991 Sierra Madre earthquake, see D. Wald, *J. Geophys. Res.* **97**, 11033 (1992). For the 1992 Landers earthquake, see D. Wald and T. Heaton, *Bull. Seismol. Soc. Am.* **84**, 668 (1994) and B. Cohee and G. Beroza, *Bull. Seismol. Soc. Am.* **84**, 692 (1994). For the 1994 Northridge earthquake, see D. Wald and T. Heaton, *U.S. Geol. Surv. Open-File Rep. 94-278* (1994).
11. D. Wald and T. Heaton, *Bull. Seismol. Soc. Am.* **84**, 668 (1994).
12. J. Brune, *J. Geophys. Res.* **75**, 4997 (1970).
13. A. Olson, J. Orcutt, G. Frazier, *Geophys. J. R. Astron. Soc.* **77**, 421 (1984).
14. J. Anderson and V. Bertero, *J. Struct. Eng. ASCE* **113** (no. 8), 1709 (1978).
15. V. Bertero, S. Mahin, R. Herrera, *Int. J. Earthquake Eng. Struct. Dyn.* **6** (no. 1), 31 (1978).
16. *Uniform Building Code* (International Conference of Building Officials, Whittier, CA, 1991).
17. *Recommended Lateral Force Requirements and Commentary* (Seismology Committee of the Structural Engineers Association of California, Sacramento, CA, 1990).
18. Critical damping is an amount just enough to cause a displaced and released structure to return to its equilibrium position without oscillation. This concept applies to a simple mass-spring system or to the vibrational modes of a complex system. Inelastic action provides additional energy dissipation.
19. V. Murty Challa and J. Hall, *Earthq. Eng. Struct. Dyn.* **23** (no. 11), 1199 (1994).
20. During the 1994 Northridge earthquake, cracks were found in welded connections of beams to columns and of columns to base plates in steel buildings. Evidence suggests that cracking occurred at low stress levels in many cases. See *Preliminary Reconnaissance Report*, Northridge Earthquake Report January 17, 1994 (Earthquake Engineering Research Institute, Oakland, CA, 1994).
21. Current design procedures generally underestimate bending and tensile loads in columns and, as a result, column splices are often made with partial penetration welds, which may have low tensile capacity.
22. The superstructure is considered to be a single rigid mass in these calculations, with the building vibrating at a pad displacement of $\frac{2}{3} D_{TM}$.
23. K. Sieh and R. Jahns, *Geol. Soc. Am. Bull.* **95**, 883 (1984).
24. *Manual of Steel Construction* (American Institute of Steel Construction, Chicago, IL, 1980).

25. We thank S. Hartzell for helpful discussions and P. Spudich, A. Frankel, and two anonymous referees for their reviews of the manuscript.

20 September 1994; accepted 17 November 1994

Earthquakes in the Los Angeles Metropolitan Region: A Possible Fractal Distribution of Rupture Size

S. E. Hough

Although there is debate on the maximum size of earthquake that is possible on any of several known fault systems in the greater Los Angeles metropolitan region, it is reasonable to assume that the distribution of earthquakes will follow a fractal distribution of rupture areas. For this assumption and an overall slip-rate for the region of approximately 1 centimeter per year, roughly one magnitude 7.4 to 7.5 event is expected to occur every 245 to 325 years. A model in which the earthquake distribution is fractal predicts that, additionally, there should be approximately six events in the range of magnitude 6.6 in this same span of time, a higher rate than has occurred in the historic record.

In recent years, geologic and geodetic investigations have made possible the evaluation of the earthquake potential for the greater Los Angeles metropolitan region, an area of about 160 km by 100 km (*1*, *2*). By evaluating available geologic and geodetic data for the total region, Dolan *et al.* (*1*) argue that 0.9 to 1.2 cm/year of slip will occur over the distribution of known and unknown faults in the region.

A report by the scientists of the Southern California Earthquake Center (SCEC) has shown that the long-term geodetic deformation rate cannot be accounted for by a continuation of the historic seismic record and has proposed three alternatives: (i) that significant aseismic slip occurs; (ii) that moderate earthquakes [that is, around magnitude (M) 6] must occur significantly more frequently than they did during the historic record; or (iii) that infrequent very large events will occur (*3*).

United States Geological Survey, Pasadena, CA 91106, USA.

In general, it is difficult to determine a priori whether a given fault system will rupture all at once, as occurred during the M 7.3 Landers earthquake in 1992 (*4*), or in isolated segments, as in 1994 during the M 6.7 Northridge earthquake (*5*). In the evaluation of seismic hazard, the distribution of expected earthquakes is critical. It is reasonable to conjecture that the long-term distribution of earthquake rupture areas will be fractal. Studies have shown that the distribution of segmentation of known fault lengths is fractal (*6*) and that the well-known log-normal distribution of earthquake magnitudes is also essentially consistent with this hypothesis (*7*). Although it has been proposed that individual fault segments will not produce a fractal distribution of events (*8*), it is commonly assumed that earthquake release in a region with numerous faults will occur by events with a log-normal distribution of magnitudes, with a maximum event size imposed for each region (*9*).